Published in final edited form as:
Bioconjug Chem. 2012 March 21; 23(3): 548–556. doi:10.1021/bc200613e.

Fibrin Specific Peptides Derived by Phage Display: Characterization of Peptides and Conjugates for Imaging

Andrew F. Kolodziej, PhD[1], **Shrikumar A. Nair, PhD**[1], **Philip Graham, PhD**[1], **Thomas J. McMurry, PhD**[1], **Robert C. Ladner, PhD**[2], **Charles Wescott, PhD**[2], **Daniel J. Sexton, PhD**[2], and **Peter Caravan, PhD**[3,4,*]

[1]EPIX Pharmaceuticals, Inc., Cambridge, MA, USA

[2]Dyax Corp., Cambridge, MA, USA

[3]Athinoula A. Martinos Center for Biomedical Imaging, Department of Radiology, Massachusetts General Hospital, Charlestown, MA

[4]Department of Radiology, Harvard Medical School, Boston, MA

Abstract

Peptides that bind to fibrin but not to fibrinogen or serum albumin were selected from phage display libraries as targeting moieties for thrombus molecular imaging probes. Three classes of cyclic peptides (cyclized via disulfide bond between two Cys) were identified with consensus sequences XArXCPY(G/D)LCArIX (Ar=aromatic, Tn6), X_2CXYYGTCLX (Tn7), and NHGCYNSYGVPYCDYS (Tn10). These peptides bound to fibrin at ~2 sites with K_d=4.1 μM, 4.0 μM, and 8.7 μM, respectively, whereas binding to fibrinogen was at least 100 – fold weaker. The peptides also bind to the fibrin degradation product DD(E) with similar affinity to that measured for fibrin. The Tn7 and Tn10 peptides bind to the same site on fibrin while the Tn6 peptides bind to a unique site. Alanine scanning identified the N- and C-terminal ends of the Tn6 and Tn7 peptides as most tolerant to modification. Peptide conjugates with either fluorescein or diethylenetriaminepentaaceto gadolinium(III) (GdDTPA) at the N-terminus were prepared for potential imaging applications and these retained fibrin binding affinity and specificity in plasma. Relaxivity and binding studies on the GdDTPA derivatives revealed that an N-terminal glycyl linker had modest effect on fibrin affinity but resulted in lower fibrin-bound relaxivity.

Keywords

Fibrin; MR Imaging; binding; peptide; phage display

Introduction

Thrombotic diseases, including atherothrombosis and stroke, are the leading cause of death in the Western world, and consequently there is considerable need for new diagnostic agents and therapies. Aberrant fibrin clot formation is associated with thrombotic disease and is initiated by the proteolysis of fibrinogen by thrombin and subsequent fibrin polymerization. Fibrin is well suited as a marker for diagnostic imaging and depot for targeted therapy as it is inexorably linked to thrombosis and is abundant in thrombi (20 – 200 μM). Several groups

Address for correspondence: Peter Caravan, A.A. Martinos Center for Biomedical Imaging, Department of Radiology, Massachusetts General Hospital, Suite 2301, 149 Thirteenth Street, Charlestown, MA 02129, Tel: +1 617 643 0193, caravan@nmr.mgh.harvard.edu.

Supporting Information Available: Additional details of the phage display study, protein preparations, binding assays, and peptide and conjugate syntheses. This material is available free of charge via the Internet at http://pubs.acs.org.

have explored fibrin specific antibodies coupled to radionuclides, nanoparticles, or incorporated into echogenic liposomes as potential contrast agents for nuclear, optical or ultrasound imaging(1). With respect to thrombolytic agents, anti-fibrin antibody conjugation has been investigated as a mechanism to enhance the specificity and reactivity of plasminogen activators(2). Additionally, conjugation of the thrombin inhibitor hirudin(3) or the Factor Xa inhibitor tick anticoagulant peptide(4) to anti-fibrin antibodies has improved the specificity and efficacy of these inhibitors, suggesting that a fibrin targeting strategy may also yield more potent antithrombotic agents.

In addition to monoclonal antibodies and the protein tissue plasminogen activator (t-PA), fibrin targeting has also been achieved through small peptides. MR contrast agents were reported that contain fibrin-specific peptide(s) conjugated to multiple gadolinium complexes. Such agents, like EP-2104R, have demonstrated efficacy in thrombus detection in a number of preclinical models of thrombosis (5–11) and recent data in human subjects has also proved promising (12). However, there has been little reported on the fibrin specific peptides themselves: their identification, specificity, cross reactivity for different fibrin binding sites, the effects of chelate conjugation, and sensitivity to amino acid substitution.

In this report we describe the strategy used to identify fibrin binding peptides with high specificity for fibrin over fibrinogen and other serum proteins. Three families of peptides were identified and the interaction of these peptides with fibrin, the soluble fibrin fragment DD(E), and fibrinogen is probed with four techniques: plate-based depletion assay, fluorescence polarization of fluorescent probes and competitive binding, isothermal calorimetry, and proton relaxation rate enhancement. The cross reactivity of these peptides for specific fibrin binding sites is also examined. The critical residues required for binding are probed using alanine and other amino acid substitutions, providing data on the critical binding motif while pointing to conjugation strategies compatible with maintaining binding affinity. The effect of fluorescein or GdDTPA conjugation on protein binding, relaxivity, and specificity is also explored. While aspects of the *in vivo* efficacy of some of these peptides as conjugates to GdDTPA have been reported, the discovery, identity and properties of these sequences have not been previously described in detail.

Experimental Procedures

Protein Preparation

Human fibrinogen was purchased from American Diagnostica. Human citrated plasma was obtained from the American Red Cross and used without further processing. The soluble fibrin fragment DD(E) was prepared as previously described(13). DD(E) used in this study contained subunits of 61 kD and 72kD, assigned to Fragments E_1 and E_2 and present in a roughly 1:1 ratio, and 180 kD (Fragment DD).

Phage Display

Tn6, Tn7, and Tn10 libraries were constructed as gene III coat protein fusions by Dyax Corporation and are described elsewhere(14). Phage selection was conducted through four rounds. Before each round, libraries were depleted of fibrinogen binders by incubating the phage with biotinylated fibrinogen bound to bead immobilized streptavidin. Fibrin binding phage were selected by contacting these non-binding phage with either fibrin (polymerized in a microtiter plate well) or to biotinylated DD(E), bound to bead immobilized streptavidin, and eluting the bound phage. Fibrin specific clones from round four were identified by phage ELISA assays as having high response against fibrin and DD(E), but low response against fibrinogen, and human serum albumin. Fibrin plates were prepared with fibrinogen (50 μL, 0.075 mg/mL) in 50 mM Tris, pH 7.4, 150 mM NaCl and 5 mM sodium citrate

polymerized in the wells of a 96 well plate (Immulon-II®) by addition of $CaCl_2$ (7 mM) and thrombin (1 U/mL) and dried overnight at 37°C).

Peptide synthesis

Peptides were synthesized by standard Fmoc solid phase protocols using rink amide or NovasynTGR-amide resin from EMD Biosciences, and prepared as C-terminal amides. Masses of all compounds were verified by electrospray mass spectrometry, and purities were >90% as assessed by HPLC. All peptides were prepared as cyclic cysteine disulfides, except where noted. Compounds are denoted by the phage library from which they were derived followed by a number to denote the sequence and then "Fl" or "Gd" if derivatized with fluorescein or GdDTPA, e.g. Tn7-3-Fl denotes a peptide derived from the Tn7 library, sequence 3, and derivatized with fluorescein. Specific sequences are listed in Tables 1 and 2. Conjugate **Tn7-3b-Gd** was reported previously (15) and in that publication is referred to as EP-782.

Fibrin Binding

The fibrin binding assay has been described previously (16). For peptide binding experiments, fibrin plates were prepared as for phage display but at higher fibrin concentration (100 μL; 2.5 mg/mL). Peptide or conjugate (1 – 100 μM; 100 μL/well), dissolved in water, were incubated in duplicate fibrin plate wells for 2 hr at 37°C. Peptide concentrations of the peptide solution added to the wells, $[Peptide]_{total}$, and in the well supernatant at equilibrium, $[Peptide]_{free}$, were quantified by RP-HPLC (C4 column) interfaced to a mass spectrometer or fluorescence detector. Bound peptide concentration was calculated as the difference $[Peptide]_{total}$ - $[Peptide]_{free}$. The dissociation constant, K_d, and number of binding sites, N_{bd}, were determined from a non-linear least-squares fit of the data, N_{bd} vs. $[Peptide]_{free}$, to a single class of sites binding model where N_{bd} is the number of molecules bound per mol fibrin (fbn), and [fbn] is the fibrin concentration, eq 1.

$$\frac{[\text{Peptide}]_{\text{bound}}}{[\text{fbn}]_{\text{total}}} = \frac{N_{bd} \times [\text{Peptide}]_{\text{free}}}{([\text{Peptide}]_{\text{free}} + K_d)} \quad (1)$$

Fluorescence polarization

Peptide and peptide conjugate binding to DD(E) was measured by a fluorescence polarization (FP) assay. The anisotropy (r_{obs}) of the fluorescein labeled peptides (Fluor•pep) binding to DD(E) (0 – 20 μM) or fibrinogen (0 – 40 μM) was measured in TBS•Ca at fixed **Tn6-2b-Fl** (0.05 μM), **Tn7-3-Fl** (0.1 μM), or **Tn10-4-Fl** (0.1 μM) concentrations, and the data were fit to a single site model(17) to obtain the dissociation constant for the DD(E) • (fluorescent peptide, "Fl") complex, K_d, and reference values for r_{bd}, the anisotropy of "Fl" when fully bound to DD(E) and r_{fr}, the anisotropy in solution.

$$r_{obs} = r_{fr} + \frac{r_{bd} - r_{fr}}{[Fl]_T} \times \frac{([DD(E)]_t + [Fl]_t + K_d) - \sqrt{([DD(E)]_t + [Fl]_t + K_d)^2 - 4[Fl]_t[DD(E)]_t}}{2} \quad (2)$$

Non-fluorescent peptide binding to DD(E) was measured by fluorescent peptide displacement. Tn6 binding: DD(E) (150 nM), **Tn6-2b-Fl** (50 nM) and peptide (0.1 – 40 μM) were mixed in TBS•Ca containing 0.01% Triton X100. Tn7 binding: DD(E) (1.5 μM) and **Tn7-3-Fl** (1 μM) and competing peptide (0.1 – 50 μM) were mixed in TBS•Ca. Sample r_{obs} (100 μL, n = 3 wells) was measured in a 96 - well microplate (Costar Cat. No. 3915), using a

Tecan Polarian 96 - well FP microplate reader (ex = 485 nm; em = 535 nm). In the presence of an inhibitor, an apparent dissociation constant for the fluorescent probe, $K_d$app, is determined, eq 3. The inhibition constant, K_i, is related to $K_d$app by eq 4 where K_d is the true dissociation constant of the fluorescent probe measured in the absence of inhibitor. K_i values were obtained by least squares fitting of the data as described elsewhere (18).

$$r_{obs}=r_{fr}+\frac{r_{bd}-r_{fr}}{[Fl]_T}\times\frac{\left([DD(E)]_t+[Fl]_t+K_d^{app}\right)-\sqrt{\left([DD(E)]_t+[Fl]_t+K_d^{app}\right)^2-4[Fl]_t[DD(E)]_t}}{2} \quad (3)$$

$$K_d^{app}=K_d\left(1+\frac{[Inhibitor]_{free}}{K_i}\right) \quad (4)$$

Isothermal Calorimetry

Peptide binding to fibrinogen or DD(E) was measured by isothermal calorimetry (ITC) carried out at MicroCal, LLC Northampton, MA. Heat changes were measured for titration of peptides **Tn6-2a** (721 μM), **Tn7-3** (1.097 mM), or **Tn10-4** (551 μM) into DD(E) (16 μM in TBS•Ca) or fibrinogen (18 μM in TBS containing 10 mM citrate). Integrated heats of binding data determined from the DD(E) titrations were fit to a single class of sites, non-cooperative binding model (19).

Relaxation rate measurements

Solvent water ^{1}H relaxation rates ($1/T_1$) were measured using a Bruker NMS 120 minispec operating at 0.47T and 37°C. Solutions (200 μL) containing 0 – 250 μM GdDTPA or **Tn7-3a-Gd** were prepared in pH 7.4 TBS with or without 30 μM fibrinogen. The fibrinogen solutions were converted to fibrin gels by addition of by addition of 4 μL of 2M $CaCl_2$ and 2 μL of 100 U/mL thrombin solution, followed by rapid mixing and then equilibration for at least 30 min. Relaxivity of the fibrin-bound complex, r_1^{bd}, and the unbound complex, r_1^{free}, were determined by a nonlinear least squares fit of equations 5 and 6 where f^{bd} and f^{free} are the mol fraction of the bound and unbound species, respectively and $1/T_1^0$ is the relaxation rate in the absence of Gd. In the absence of fibrin, $f^{bd}=0$, and r_1^{free} is determined from a linear fit of $1/T_1$ vs [Gd].

$$\frac{1}{T_1}=\frac{1}{T_1^0}+\left(f^{free}\,r_1^{free}+f^{bd}\,r_1^{bd}\right)\times[Gd];\quad f^{free}+f^{fd}=1 \quad (5)$$

$$f^{bd}=\frac{([Gd]+N_{bd}[fbn]+K_d)-\sqrt{([Gd]+N_{bd}[fbn]+K_d)^2-4[Gd]N_{bd}[fbn]}}{2[Gd]} \quad (6)$$

Supporting Information Available

Additional description of phage display screening and selection procedures (including phage binding and selectivity assays measured by ELISA), synthesis of peptides and conjugates, and fibrin, fibrinogen, and DD(E) binding assays are provided. This material is available free of charge via the internet at http://pubs.acs.org.

Results

Phage Display—Our strategy for isolating fibrin specific peptides by phage display relied upon three key elements: alternative target presentations, negative selection to remove fibrinogen binders, and selection from multiple phage libraries. The target fibrin was presented in two different forms, as polymerized, gelled fibrin and as the plasmin degradation product DD(E). DD(E) is a useful soluble model of the insoluble fibrin polymer and has been shown to retain many epitopes unique to fibrin, including the D-D and D–E domain interfaces, factor XIIIa crosslinks on the γ-chain, and a fibrin specific t-PA binding site(20). Fibrin was presented as a thin dried film, a format that minimized non-specific phage retention, while maintaining fibril structures similar to those of wet clots(21). The fibrin clots were stable to the phage selection procedures with negligible loss of protein from the plate upon repeated washing, and bound fibronectin (IC_{50} = 4.9 ± 1.9 nM, ELISA data not shown) with affinity similar to previously reported values(22). The high degree of structural similarity between fibrin and fibrinogen necessitated a negative screen to remove fibrinogen-binding phage which was repeated before each round of panning to promote removal of fibrinogen binders potentially carried over and amplified from the previous round.

Fibrin specific phage were obtained from three phage libraries, all containing cysteine disulfide cross-linked sequences: $X_3CX_4CX_3$ (Tn6 library), $X_3CX_5CX_3$ (Tn7) and $X_3CX_8CX_3$ (Tn10) where X was variagated. These selectants were identified after four rounds of selection by phage ELISA, as yielding high responses on the immobilized DD(E) and fibrin, but low background signals with immobilized fibrinogen and HSA. Sequencing of these clones (>20/library) yielded a single consensus sequence for each library. The two unique sequences obtained from the Tn6 library, QWECPYGLCWIQ and WFHCPYDLCHIL together conformed to a XArXCPY(G/D)LCArIX (Ar = aromatic) consensus. The ten unique Tn7 sequences aligned to a X_2CXYYGTCLX sequence where the YYGT sequence was strictly conserved along with a preference for polar amino acids (H, D, S, and N) at the lone variable position within the disulfide loop. A single sequence was obtained from the Tn10 selection, NHGCYNSYGVPYCDYS, which contained a ‘SYGV’ motif that appeared to be functionally homologous to the ‘YYGT’ motif of the Tn7 sequence. Sequences for the Tn6, Tn7 and Tn10 peptides were compared against the protein sequence database, but no proteins having a functional role related to fibrin(ogen) recognition or haemostasis were found. The Tn7 consensus sequence YYGT is similar to a surface exposed loop on the fibrin(ogen) gamma chain YYQGGT, γ(348–353), and to the sequence SYGT, α(257–261), but no functional role has been ascribed to these sequences.

Analysis of Peptide Binding to Fibrin, DD(E) and Fibrinogen

Fibrin Binding Measurements—Peptides corresponding to representative selected sequences from the Tn6, Tn7 and Tn10 libraries were synthesized, and binding to fibrin films was measured in a microtiter plate equilibrium binding assay. This method allowed for rapid diffusion of the peptide into the fibrin gel and equilibrium was reached within 45 minutes, as assessed by time courses of peptide uptake into fibrin. Peptides derived from the two Tn6 sequences, **Tn6-1** and **Tn6-2a** (truncation of the N-terminal glutamine from the phage derived sequence **Tn6-2b** increased affinity two fold and improved peptide solubility), bound to fibrin with similar affinities, Table 1 and Figure 1. A representative Tn7 peptide, **Tn7-3,** and the Tn10 peptide **Tn10-4** also bound with affinities in the low micromolar range, Table 1. Notably, all peptides bound to approximately two binding sites per fibrin monomer, consistent with the dimeric structure of this protein. Peptide affinities, however, were considerably lower than expected based on phage ELISA where very tight binding was observed. This affinity difference was probably due to avidity effects arising

from polyvalent peptide display (up to five peptides per phage), although some additional affinity due to the native phage protein cannot be ruled out. No fibrin binding was observed for a modified Tn7 peptide (sequence LPCDYYG**A**CLD), where the single threonine residue was replaced with alanine. This observation highlighted the importance of this consensus residue in fibrin binding and also indicated that binding measurements were not complicated by peptide entrapment.

Fluorescence Polarization—Selectivity and affinity of the Tn6, Tn7 and Tn10 peptides to DD(E) and fibrinogen was measured by a fluorescence polarization assay using N-terminal fluorescein conjugates of these peptides. Affinity of the fluorescein derivatives of the Tn7 and Tn10 peptides to DD(E) was low micromolar, similar to that of the parent peptides to fibrin or DD(E), Table 1 and Figure 2. On the other hand, affinity of **Tn6-2b-Fl** for DD(E) was higher with K_d = 0.057 μM, Figure 2. Binding was saturable for all 3 fluorescent probes.

Binding of unlabeled Tn6 and Tn7 peptides to DD(E) was measured by a competition assay (Figure 3), and compared to the fluorescein labeled analogs. **Tn7-3** displaced **Tn7-3-Fl** with K_i = 2.8 μM, an affinity similar to the fluorescein labeled probe. However, **Tn6-2a** displaced **Tn6-2b-Fl** with K_i = 0.9 μM, a 16-fold reduction in binding affinity compared to the fluorescent probe, indicating that the aromatic fluorescein moiety enhanced the affinity of this peptide (Figure 3). Likewise, **Tn6-1**, the other Tn6 sequence type, displaced **Tn6-2b-Fl** with K_i = 3.1 μM. The DD(E) competition assay also established that the Tn6 and Tn7 peptides bind to separate sites on DD(E), since **Tn6-1** and **Tn6-2a** failed to reduce **Tn7-3-Fl** anisotropy, nor did the Tn7 peptide **Tn7-3** displace **Tn6-2b-Fl**. However **Tn10-4** did displace **Tn7-3-Fl** (K_i = 3.5 ± 0.3 μM) with affinity similar to **Tn7-3** indicating that peptide **Tn10-4** also binds to the Tn7 site. The Tn10 peptide could not displace the Tn6 probe at concentrations up to 100 μM.

Despite some functional sequence homology, in that the DYYGT sequence in Tn7 has similarity to the NSYGV sequence in Tn10, the DYYGT sequence cannot functionally substitute for the associated residues in the Tn10 sequence. Four hybrid peptides of the Tn10 peptide were prepared, focusing on the N^6, S^7 and V^9 positions. Replacement of S^7 with tyrosine had little effect, while substitution of either N^6 with aspartate, V^9 with threonine, or all three residues together sharply reduced binding (Table 2). Conversely, replacement of T^8 in **Tn7-3** with its β-branched analog valine reduced binding to DD(E) 10 – fold. Despite binding to the same site, the residue preference and orientation is exquisitely sensitive to constraints of the disulfide architecture.

The fluorescein labeled peptides exhibited strong selectivity for DD(E) over fibrinogen when anisotropy changes were examined. The data for **Tn6-2b-Fl** (Figure 2a) fit to a K_d = 22 μM, 400 – fold weaker than to DD(E). The fibrinogen affinity of the unlabeled peptide was much weaker since the fluorescein moiety enhanced fibrinogen binding, as observed with DD(E). The Tn6 data were shifted only slightly in the presence of a 100-fold excess of the unlabeled **Tn6-1**, see Supporting Information. When binding of **Tn6-1** (0 – 50 μM) to fibrinogen was assessed at a fixed concentration of fibrinogen (7 μM) and **Tn6-2b-Fl** (0.1 μM), displacement was partial and did not change for **Tn6-1** concentrations >20 μM. Overall, the data indicated that **Tn6-1** competed poorly with **Tn6-2b-Fl**, and a K_d > 200 μM was estimated. For **Tn7-3-Fl**, the anisotropy increased in the presence of fibrinogen, but the change was small and nearly linear with increasing fibrinogen concentration, suggesting that the anisotropy effects were due largely to increasing viscosity at high fibrinogen concentrations (Figure 2b). Consistent with a non-specific effect, the anisotropy increase was not reversed by competition, as anisotropy data obtained in the presence of a 100-fold (100 μM) excess of unlabeled Tn7 peptide (**Tn7-3**) were nearly identical, see Supporting

Information. In summary, both the Tn6 and Tn7 sequences have a ~100 – fold selectivity for DD(E) over fibrinogen, as measured by this method.

Isothermal Calorimetry—Isothermal calorimetry (ITC) data for binding of the Tn6, Tn7 and Tn10 peptides to DD(E) and fibrinogen confirmed the affinity and specificity measurements obtained by fluorescence polarization (Figure 4). Data for these peptides titrated into a DD(E) solution displayed exothermic binding heats and it appeared at the end of the titrations that nearly all DD(E) binding sites had been occupied by ligand. Binding constants for all three peptides were very close to the values obtained from the fluorescence polarization assay, Table 1. In addition, the data fit to stoichiometries of 2 binding events per DD(E), indicating that, like fibrin, the peptides bind independently to two binding sites on DD(E).

Data for **Tn6-2a** titrated with fibrinogen displayed very small, constant heat effects that were comparable to the control, indicating that any binding interaction between the Tn6 peptide and fibrinogen is weak with K_d > 50 μM. The data for **Tn7-3** and **Tn10-4** titrated with fibrinogen were more complex. Addition of these peptides to concentrated fibrinogen solutions resulted in fibrinogen aggregation, and formation of a watery gel. However, the heat released with each **Tn7-3** addition to fibrinogen was very small compared to those observed with DD(E) and probably arose from fibrinogen aggregation. In a separate experiment (see supplemental data), **Tn7-3** was added to a fibrinogen solution (5 mg/mL), and the scattered light intensity, measured by absorbance at 350 nm, increased in 10 min from 0.04 to 0.32 in a sigmoidal transition, confirming that peptide addition induced aggregation of the fibrinogen. This phenomenon did not occur in citrated human plasma, presumably due to lower fibrinogen concentration, and an overall high protein concentration that would disfavor fibrinogen self-association. The titration calorimetry data did not fit to a standard binding model, but it can be inferred that **Tn7-3** affinity to fibrinogen is very weak, with $K_d \gg 20$ μM. Very similar results were obtained for **Tn10-4**, consistent with the prior observation that it binds to the same site on fibrin as **Tn7-3**.

Peptide Binding Determinants—To identify residues in the Tn6 and Tn7 sequences required for fibrin binding, each position (except the cysteines) was systematically changed to alanine (Table 2), and tested for binding to DD(E) in the fluorescence polarization assay. The two Tn6 peptides bind in a similar fashion with residues P^5, Y^6, and L^8 within the PY(G/D)L consensus sequence exhibiting particular sensitivity to substitution and conferring most of the binding affinity. In addition, alanine substitutions at the residues flanking the C-terminal cysteine, especially the aromatic W^{10}/H^{10} and hydrophobic I^{11} sites, led to much weaker binding than similar substitutions at the N-terminal flanking region, indicating that the C-terminus contributes more to the peptide-fibrin interaction. For the Tn7 sequence, a substantial reduction in binding was observed for changes at Y^6 and T^8, highlighting the critical role of these conserved residues for fibrin binding. Reduction of hydrophobicity at L^{10} also lowered binding affinity, indicating a secondary contribution from this residue. Substitution of the other exocyclic residues or at the D^4 position had little effect on binding, consistent with the greater variability observed at these sites in the sequences obtained by phage display.

The conformation as maintained by the cyclic disulfide was also critical for high affinity binding. Reduction of the disulfide in **Tn6-1** and **Tn7-3** with excess tris(2-carboxyethyl)phosphine (TCEP), or substitution of the cysteines with serine in **Tn7-3** abrogated binding to DD(E) and fibrin completely. Even modulation of the disulfide conformation reduced binding considerably. For example, in **Tn6-1** either L-cysteine replaced with D-cysteine, or in **Tn7-3**, substitution of C^3 with penicillamine (β, β′-dimethylcysteine) resulted in non-binding peptides.

Gd-DTPA Derivatives—Prototype fibrin targeted MRI contrast agents were synthesized by conjugating the paramagnetic gadolinium chelate Gd(DTPA) to the N-terminus of **Tn6-1** and **Tn7-3** via 0 – 2 glycyl linkers. Despite the addition of the large Gd(DTPA) moiety, the conjugates **Tn6-1-Gd** and **Tn7-3b-Gd** bound to DD(E) and to fibrin in TBS buffer with similar affinity to the parent peptides (Table 1). When binding to fibrin was measured in human citrated plasma, the fibrin affinity was only decreased 2–3-fold: **Tn6-1-Gd** bound to fibrin with K_d = 3.1 ± 0.3 μM and 2.3 ± 0.1 sites per fibrin monomer, while **Tn7-3b-Gd** bound with K_d = 8.4 ± 0.5 μM and 1.8 ± 0.1 sites/fibrin. For the Tn7 peptide, both peptide derivatization and plasma binding contributed roughly equally to the observed lower binding affinity, as the K_d values in buffer (Table 1) were intermediate between those measured for the peptide in TBS and for the conjugate in plasma. No measurable fibrin binding was observed for a scrambled version of **Tn7-3b-Gd** (sequence DTPA-GYLCGDYTLCPD-NH_2) (15).

The presence of the paramagnetic Gd(III) moiety allows estimation of fibrin affinity using the proton relaxation enhancement (PRE) effect. The longitudinal relaxation rate ($1/T_1$) of solvent water increases if the peptide conjugate binds to protein. Solutions containing varying concentrations of **Tn7-3a-Gd** were prepared either in TBS or in TBS containing 30 μM fibrinogen. The fibrinogen solutions were converted to fibrin gels by addition of $CaCl_2$ and thrombin. Figure 5 shows that $1/T_1$ is higher for **Tn7-3a-Gd** in the presence of fibrin compared to buffer only. The $1/T_1$ data is nonlinear for the data in fibrin indicative of a saturable binding event. A control study showed no enhancement of $1/T_1$ for GdDTPA in fibrin gel compared to GdDTPA in buffer demonstrating a specific interaction between **Tn7-3a-Gd** and fibrin.

The relaxivity of **Tn7-3a-Gd** bound to fibrin was 25.5 ± 0.7 $mM^{-1}s^{-1}$ at 37 °C, 0.47T which is significantly higher than that for **Tn7-3b-Gd** under the same conditions (14.9 $mM^{-1}s^{-1}$), whereas the relaxivity in the absence of fibrin was similar for the two compounds: 8.6 ± 0.3 and 10.1 $mM^{-1}s^{-1}$ for **Tn7-3a-Gd** and **Tn7-3b-Gd** respectively (15). The increased fibrin-bound relaxivity of **Tn7-3a-Gd** can be attributed to the lack of the glycyl linker. The GdDTPA moiety is coupled directly to the leucine N-terminus resulting in restricted rotational motion when the compound binds fibrin. While placing the large GdDTPA group close to the conserved portion of the binding sequence could be expected to reduce affinity, in this case affinity was similar regardless of the spacer, while there was a clear advantage to minimizing the spacer length to obtain optimal relaxivity properties.

Discussion

We describe three families of small peptides that discriminate in their binding between two distinct conformational states of fibrinogen, the soluble protein central to haemostasis, and fibrin, the polymerized form that provides the structural network of thrombi. These cyclic peptide classes were obtained by phage display from three disulfide constrained libraries that exhibited high binding affinity to fibrin, in the low micromolar range, and >100-fold selectivity for fibrin over fibrinogen. Fibrin and DD(E) binding was assessed by four independent methods: plate-based depletion, fluorescence polarization and probe displacement, isothermal calorimetry, and proton relaxation enhancement assays. No evidence was observed for specific fibrinogen binding in these assays. Peptide binding to DD(E) was comparable to fibrin, which is evidence that DD(E) is a good structural model for fibrin, since the neo-epitopes recognized by these peptides are structurally maintained and accessible in both proteins. It is remarkable that this degree of specificity is conferred by such short peptides, especially given that much of the overall conformation is expected to be similar between fibrin and fibrinogen(23). A few residues on each peptide were responsible for fibrin recognition, and these hot spots corresponded to conserved residues highlighted in

the phage display results. A peptide architecture rigidified by disulfide bonds also proved crucial to holding the peptides in a high affinity conformation.

All peptides bound to two sites per fibrin monomer, consistent with the dimeric structure of fibrin. These peptides potentially recognize new surfaces formed by interdomain contacts present in fibrin, but absent in fibrinogen, or they bind to surfaces exposed by domain movements induced by fibrin polymerization. Identification of the binding site location may help elucidate conformational differences between fibrin and fibrinogen, and is ongoing. The fibrin N-termini, well-known epitopes recognized by fibrin-specific antibodies(24) but absent in DD(E), as well as the 'a' and 'b' holes, fully or partially occupied in fibrin, can be ruled out. The Tn7/Tn10 binding site is of particular interest as it may be involved in fibrin polymerization, as suggested by these peptides' ability to induce fibrinogen self-association and gelation. By binding at an interface, such as between the D-E or D-D domains, it may stabilize a complex of three fibrinogen monomers oriented to form a DD(E)-like structure that has similar surface interactions between the monomers, but is of course absent any covalent crosslinks or a′ and 'b' site occupation. Such peptide-fibrinogen complexes, even if present at low concentration, evidently speed the rate of protofibril nucleation, the rate determining step in (thrombin independent) fibrin gel assembly (25), seeding further aggregation.

The N-terminus of all three classes of peptide can be modified with either a fluorophore or a GdDTPA moiety without significant loss of affinity, provided a spacer (e.g. glycine) is introduced at the N-terminus. The GdDTPA conjugates of the Tn6 and Tn7 peptides both retained excellent *in vitro* selectivity and high fibrin binding affinity in plasma, despite the presence of fibrinogen at a concentration equimolar to fibrin and 660 μM HSA. The low μM binding constants are within the range required for fibrin targeting *in vivo*, since the high concentration of fibrin in human thrombi (25 – 200 μM) should promote binding of these compounds under physiological conditions. For the conjugates here, we conservatively expect a percent bound of >80% resulting in a fibrin:plasma ratio of >4:1. Moreover, the two peptide binding sites per fibrin molecule doubles the effective capacity, providing an added enhancement in imaging sensitivity.

The feasibility of this approach was recently demonstrated with imaging agents based on the Tn6 peptide termed EP-1873 and EP-2104R (16, 26), and on the Tn7 peptide (15, 27, 28). These compounds contain a modified form of the parent Tn6 (or Tn7) peptide and have four Gd chelates attached. The Gd-modified peptides, both Tn6 and Tn7, maintain >100-fold specificity for fibrin over fibrinogen and >1000-fold specificity for fibrin over serum albumin (16, 27). These agents were used in swine models of coronary thrombosis (5, 7), pulmonary embolism (7, 8, 10), atrial thrombus (8), and cerebral venous sinus thrombosis (11), rabbit models of ruptured atherosclerotic plaque (26) and carotid thrombosis (29), and rat models of ischemic stroke (30, 31). Recent clinical trial data with a fibrin-targeted gadolinium-based probe, EP-2104R, indicated that this probe can identify thrombi in the heart chambers, carotid arteries, or aortic arch (32). The positive image contrast persists for hours (12), indicating a slow off-rate of the peptide from the clot due to the high concentration of fibrin binding sites.

These peptides could also find applications in other modalities. Fluorescence imaging of fibrin is readily achieved with the fluorescein derivatives described herein and such probes may find use in optical imaging applications such as intravital microscopy (33). Alternatively, these peptides could be coupled to plasminogen activators to enhance the clot specificity of fibrinolytic treatments, or conjugated to antithrombotic compounds to inhibit active clotting factors associated with pathological thrombi while minimizing systemic side effects. These small peptides are easily synthesized and may be readily conjugated without

loss of function, thus providing a new and more flexible approach to fibrin targeting than any previous strategies.

CONCLUSIONS

Phage display, with a preselection to remove fibrinogen and serum protein binders, is a powerful tool to identify fibrin specific peptides. Three classes of disulfide bridged cyclic peptides were identified that bind to two unique sites on fibrin and DD(E). The peptides show only weak nonspecific affinity to fibrinogen or plasma proteins. Alanine and other point substitutions identify the amino acids critical to fibrin binding within these short peptides. The peptides are readily modified at the N-terminus without affinity loss and represent useful building blocks to create conjugates for fibrin-targeted imaging or therapy.

Supplementary Material

Refer to Web version on PubMed Central for supplementary material.

Acknowledgments

This work was supported in part by Award Number R21NS075627 from the National Institute Of Neurological Disorders And Stroke to P.C.

References

1. Morawski AM, Lanza GA, Wickline SA. Targeted contrast agents for magnetic resonance imaging and ultrasound. Curr Opin Biotechnol. 2005; 16:89–92. [PubMed: 15722020]
2. Runge MS, Harker LA, Bode C, Ruef J, Kelly AB, Marzec UM, Allen E, Caban R, Shaw SY, Haber E, Hanson SR. Enhanced thrombolytic and antithrombotic potency of a fibrin-targeted plasminogen activator in baboons. Circulation. 1996; 94:1412–22. [PubMed: 8823001]
3. Peter K, Graeber J, Kipriyanov S, Zewe-Welschof M, Runge MS, Kubler W, Little M, Bode C. Construction and functional evaluation of a single-chain antibody fusion protein with fibrin targeting and thrombin inhibition after activation by factor Xa. Circulation. 2000; 101:1158–64. [PubMed: 10715263]
4. Hagemeyer CE, Tomic I, Jaminet P, Weirich U, Bassler N, Schwarz M, Runge MS, Bode C, Peter K. Fibrin-targeted direct factor Xa inhibition: construction and characterization of a recombinant factor Xa inhibitor composed of an anti-fibrin single-chain antibody and tick anticoagulant peptide. Thromb Haemost. 2004; 92:47–53. [PubMed: 15213844]
5. Botnar RM, Buecker A, Wiethoff AJ, Parsons EC Jr, Katoh M, Katsimaglis G, Weisskoff RM, Lauffer RB, Graham PB, Gunther RW, Manning WJ, Spuentrup E. In vivo magnetic resonance imaging of coronary thrombosis using a fibrin-binding molecular magnetic resonance contrast agent. Circulation. 2004; 110:1463–6. Epub 2004 Jul 6. [PubMed: 15238457]
6. Sirol M, Fuster V, Badimon JJ, Fallon JT, Moreno PR, Toussaint JF, Fayad ZA. Chronic thrombus detection with in vivo magnetic resonance imaging and a fibrin-targeted contrast agent. Circulation. 2005; 112:1594–600. Epub 2005 Sep 6. [PubMed: 16145001]
7. Spuentrup E, Buecker A, Katoh M, Wiethoff AJ, Parsons EC, Botnar RM, Weisskoff RM, Graham PB, Manning WJ, Gunther RW. Molecular magnetic resonance imaging of coronary thrombosis and pulmonary emboli with a novel fibrin-targeted contrast agent. Circulation. 2005; 111:1377–1382. [PubMed: 15738354]
8. Spuentrup E, Fausten B, Kinzel S, Wiethoff AJ, Botnar RM, Graham PB, Haller S, Katoh M, Parsons EC, Manning WJ, Busch T, Gunther RW, Buecker A. Molecular magnetic resonance imaging of atrial clots in a swine model. Circulation. 2005; 112:396–399. [PubMed: 16009790]
9. Spuentrup E, Katoh M, Wiethoff AJ, Parsons EC, Botnar RM, Mahnken AH, Gunther RW, Buecker A. Molecular magnetic resonance imaging of pulmonary emboli with a fibrin-specific contrast agent. Am J Resp Crit Care Med. 2005; 172:494–500. [PubMed: 15937292]

10. Spuentrup E, Katoh M, Buecker A, Fausten B, Wiethoff AJ, Wildberger JE, Haage P, Edward CP, Botnar RM, Graham PB, Vettelsehoss M, Gunther RW. Molecular MR imaging of human thrombi in a swine model of pulmonary embolism using a fibrin-specific contrast agent. Invest Radiol. 2007; 42:586–595. [PubMed: 17620942]
11. Stracke CP, Katoh M, Wiethoff AJ, Parsons EC, Spangenberg P, Spuntrup E. Molecular MRI of cerebral venous sinus thrombosis using a new fibrin-specific MR contrast agent. Stroke. 2007; 38:1476–1481. [PubMed: 17379818]
12. Spuentrup E, Botnar RM, Wiethoff AJ, Ibrahim T, Kelle S, Katoh M, Oezgun M, Nagel E, Vymazal J, Graham PB, Gunther RW, Maintz D. MR imaging of thrombi using EP-2104R, a fibrin-specific contrast agent: initial results in patients. Eur Radiol. 2008; 18:1995–2005. [PubMed: 18425519]
13. Moskowitz KA, Budzynski AZ. The (DD)E complex is maintained by a composite fibrin polymerization site. Biochemistry. 1994; 33:12937–44. [PubMed: 7524657]
14. Sato AK, Sexton DJ, Morganelli LA, Cohen EH, Wu QL, Conley GP, Streltsova Z, Lee SW, Devlin M, DeOliveira DB, Enright J, Kent RB, Wescott CR, Ransohoff TC, Ley AC, Ladner RC. Development of mammalian serum albumin affinity purification media by peptide phage display. Biotechnol Prog. 2002; 18:182–92. [PubMed: 11934284]
15. Nair S, Kolodziej AF, Bhole G, Greenfield MT, McMurry TJ, Caravan P. Monovalent and Bivalent Fibrin-specific MRI Contrast Agents for Detection of Thrombus. Angew Chem Int Ed Engl. 2008; 47:4918–21. [PubMed: 18496805]
16. Overoye-Chan K, Koerner S, Looby RJ, Kolodziej AF, Zech SG, Deng Q, Chasse JM, McMurry TJ, Caravan P. EP-2104R: a fibrin-specific gadolinium-based MRI contrast agent for detection of thrombus. J Am Chem Soc. 2008; 130:6025–39. [PubMed: 18393503]
17. Burke, T.; Bolger, R.; Checovich, W.; Lowery, R. Measurement of Peptide Binding Affinities Using Fluorescence Polarization. In: Kay, BK.; Winter, J.; McCafferty, J., editors. Phage Display of Peptides and Proteins: A Laboratory Manual. Academic Press; San Diego, CA: 1996. p. 305-326.
18. Feng S, Kasahara C, Rickles RJ, Schreiber SL. Specific interactions outside the proline-rich core of two classes of Src homology 3 ligands. Proc Natl Acad Sci U S A. 1995; 92:12408–15. [PubMed: 8618911]
19. Indyk L, Fisher HF. Theoretical aspects of isothermal titration calorimetry. Methods Enzymol. 1998; 295:350–64. [PubMed: 9750227]
20. Yakovlev S, Makogonenko E, Kurochkina N, Nieuwenhuizen W, Ingham K, Medved L. Conversion of fibrinogen to fibrin: mechanism of exposure of tPA- and plasminogen-binding sites. Biochemistry. 2000; 39:15730–41. [PubMed: 11123898]
21. Tymkewycz PM, Creighton-Kempsford LJ, Hockley D, Gaffney PJ. Screening for fibrin specific monoclonal antibodies: the development of a new procedure. Thromb Haemost. 1992; 68:48–53. [PubMed: 1514172]
22. Makogonenko E, Tsurupa G, Ingham K, Medved L. Interaction of fibrin(ogen) with fibronectin: further characterization and localization of the fibronectin-binding site. Biochemistry. 2002; 41:7907–13. [PubMed: 12069579]
23. Doolittle RF. Structural basis of the fibrinogen-fibrin transformation: contributions from X-ray crystallography. Blood Rev. 2003; 17:33–41. [PubMed: 12490209]
24. Hui KY, Haber E, Matsueda GR. Monoclonal antibodies to a synthetic fibrin-like peptide bind to human fibrin but not fibrinogen. Science. 1983; 222:1129–32. [PubMed: 6648524]
25. Hantgan R, McDonagh J, Hermans J. Fibrin assembly. Ann N Y Acad Sci. 1983; 408:344–66. [PubMed: 6135380]
26. Botnar RM, Perez AS, Witte S, Wiethoff AJ, Laredo J, Hamilton J, Quist W, Parsons EC Jr, Vaidya A, Kolodziej A, Barrett JA, Graham PB, Weisskoff RM, Manning WJ, Johnstone MT. In vivo molecular imaging of acute and subacute thrombosis using a fibrin-binding magnetic resonance imaging contrast agent. Circulation. 2004; 109:2023–9. Epub 2004 Apr 5. [PubMed: 15066940]

27. Zhang Z, Kolodziej AF, Greenfield MT, Caravan P. Heteroditopic binding of magnetic resonance contrast agents for increased relaxivity. Angew Chem Int Ed Engl. 2011; 50:2621–4. [PubMed: 21370351]

28. Zhang Z, Kolodziej AF, Qi J, Nair SA, Wang X, Case AW, Greenfield MT, Graham PB, McMurry TJ, Caravan P. Effect of Peptide-Chelate Architecture on Metabolic Stability of Peptide-based MRI Contrast Agents. New J Chem. 2010; 2010:611–616.

29. Sirol M, Aguinaldo JG, Graham PB, Weisskoff R, Lauffer R, Mizsei G, Chereshnev I, Fallon JT, Reis E, Fuster V, Toussaint JF, Fayad ZA. Fibrin-targeted contrast agent for improvement of in vivo acute thrombus detection with magnetic resonance imaging. Atherosclerosis. 2005; 182:79–85. Epub 2005 Mar 25. [PubMed: 16115477]

30. Uppal R, Catana C, Ay I, Benner T, Sorensen AG, Caravan P. Bimodal Thrombus Imaging: Simultaneous PET/MR Imaging with a Fibrin-targeted Dual PET/MR Probe--Feasibility Study in Rat Model. Radiology. 2011; 258:812–20. [PubMed: 21177389]

31. Uppal R, Ay I, Dai G, Kim YR, Sorensen AG, Caravan P. Molecular MRI of intracranial thrombus in a rat ischemic stroke model. Stroke. 2010; 41:1271–7. [PubMed: 20395615]

32. Vymazal J, Spuentrup E, Cardenas-Molina G, Wiethoff AJ, Hartmann MG, Caravan P, Parsons EC Jr. Thrombus imaging with fibrin-specific gadolinium-based MR contrast agent EP-2104R: results of a phase II clinical study of feasibility. Invest Radiol. 2009; 44:697–704. [PubMed: 19809344]

33. Falati S, Gross P, Merrill-Skoloff G, Furie BC, Furie B. Real-time in vivo imaging of platelets, tissue factor and fibrin during arterial thrombus formation in the mouse. Nat Med. 2002; 8:1175–81. Epub 2002 Sep 16. [PubMed: 12244306]

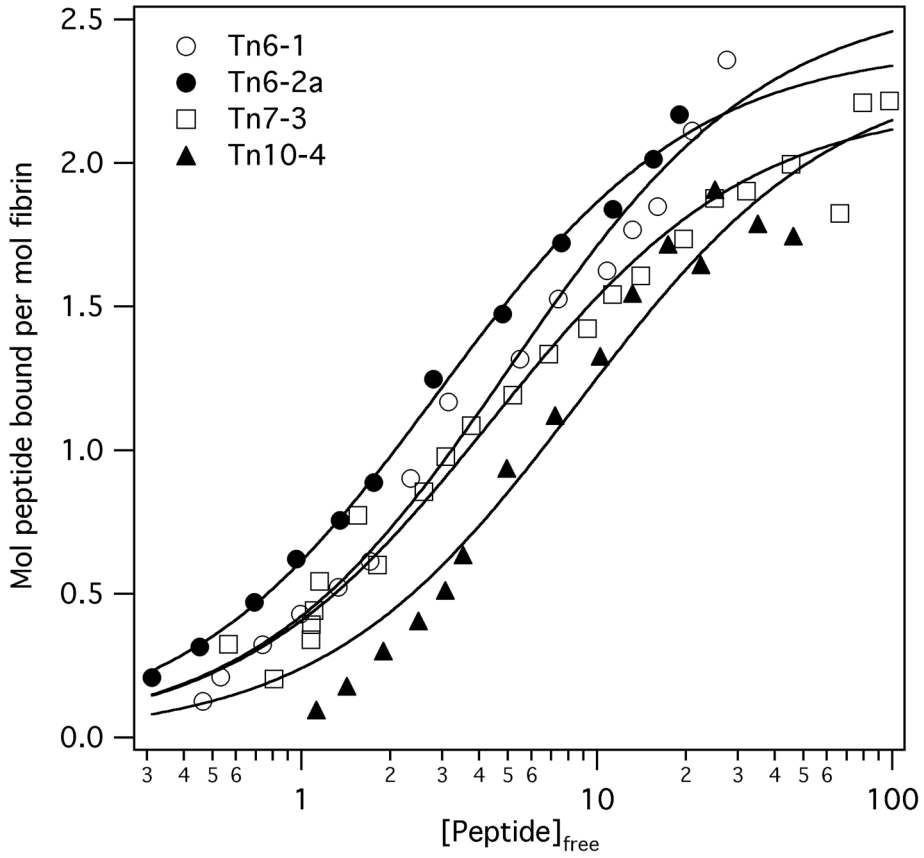

Figure 1.

Fibrin binding data for the **Tn6-1**, **Tn6-2a**, **Tn7-3**, and **Tn10-4** peptides, and fits to single class-of-sites binding model demonstrating low micromolar affinity and binding to two sites on fibrin. Standard errors for individual points were <15% of the ordinate value.

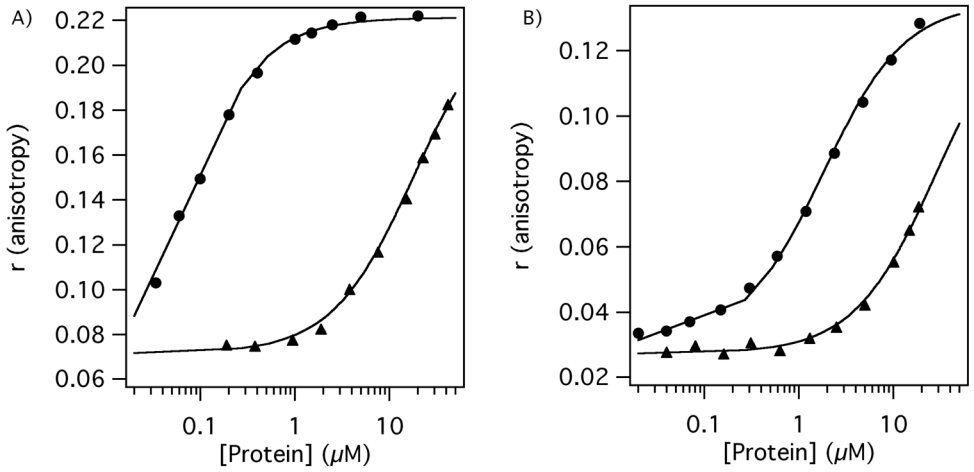

Figure 2.

Binding of fluorescein labeled peptides **Tn6-2b-Fl** (0.050 μM, panel A) and **Tn7-3-Fl** (0.100 μM, panel B) to DD(E) (closed circles) and to fibrinogen (closed triangles) demonstrating high selectivity for DD(E) over fibrinogen.

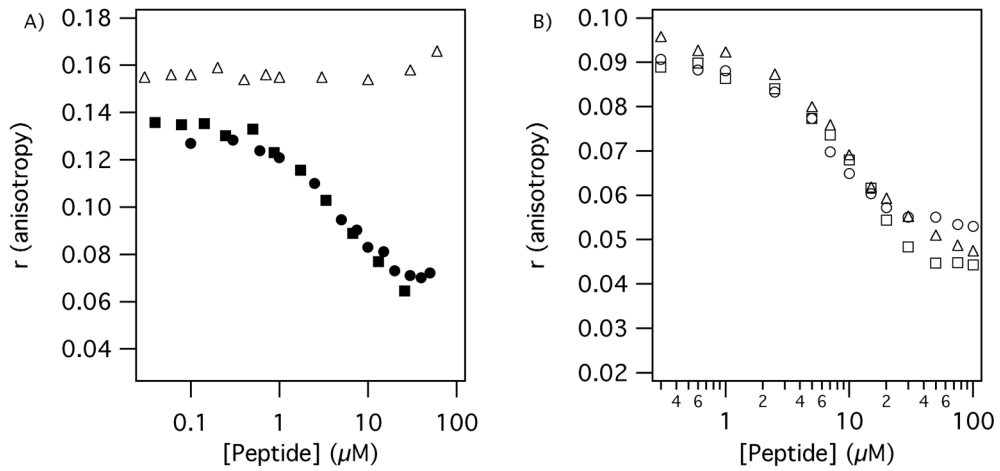

Figure 3.

DD(E) (1.5 μM) binding measured by displacement of fluorescent probes. A) **Tn6-2b-Fl** (0.050 μM) is displaced by Tn6 compounds **Tn6-1** (filled circles) and **Tn6-1-Gd** (filled squares) but not by Tn10 peptide **Tn10-4** (open triangles). B) **Tn7-3-Fl** (1.0 μM) is displaced by Tn7 compounds **Tn7-3** (open circles) and **Tn7-3b-Gd** (open squares) and by the Tn10 peptide **Tn10-4** (open triangles) indicating the Tn7 and Tn10 binding site is the same.

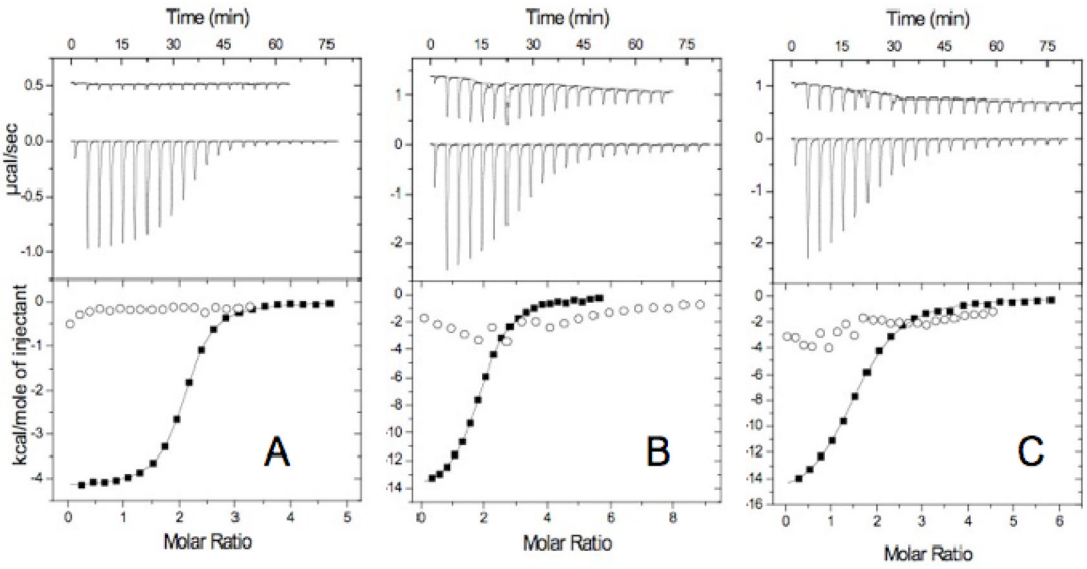

Figure 4.

Calorimetry data for peptide binding to fibrinogen and DD(E). Upper panels: raw heat data measured over a series of injections (Fibrinogen, top curves; DD(E) lower curves). Lower panels: integrated heat per mol injected peptide plotted against the molar ratio of added peptide to protein (Fibrinogen binding, open circles, no fit; DD(E) binding, closed boxes with fit). Conditions for titrations and data were as follows. Figure 4a: **Tn6-2a** (721 μM) into 28.5 μM fibrinogen, 10 μl/inj. and 24.7 μM DD(E), 5 μL/inj. Figure 4b: 1.099 mM **Tn7-3** into 17.5 μM fibrinogen, 10 μl/inj. and 16 μM DD(E) 10 μl/inj. Figure 4c: 462 μM **Tn10-4** into 17.5 μM fibrinogen, 10 μl/inj. and 551 μM **Tn10-4** into 16 μM DD(E), 10 μl/inj.

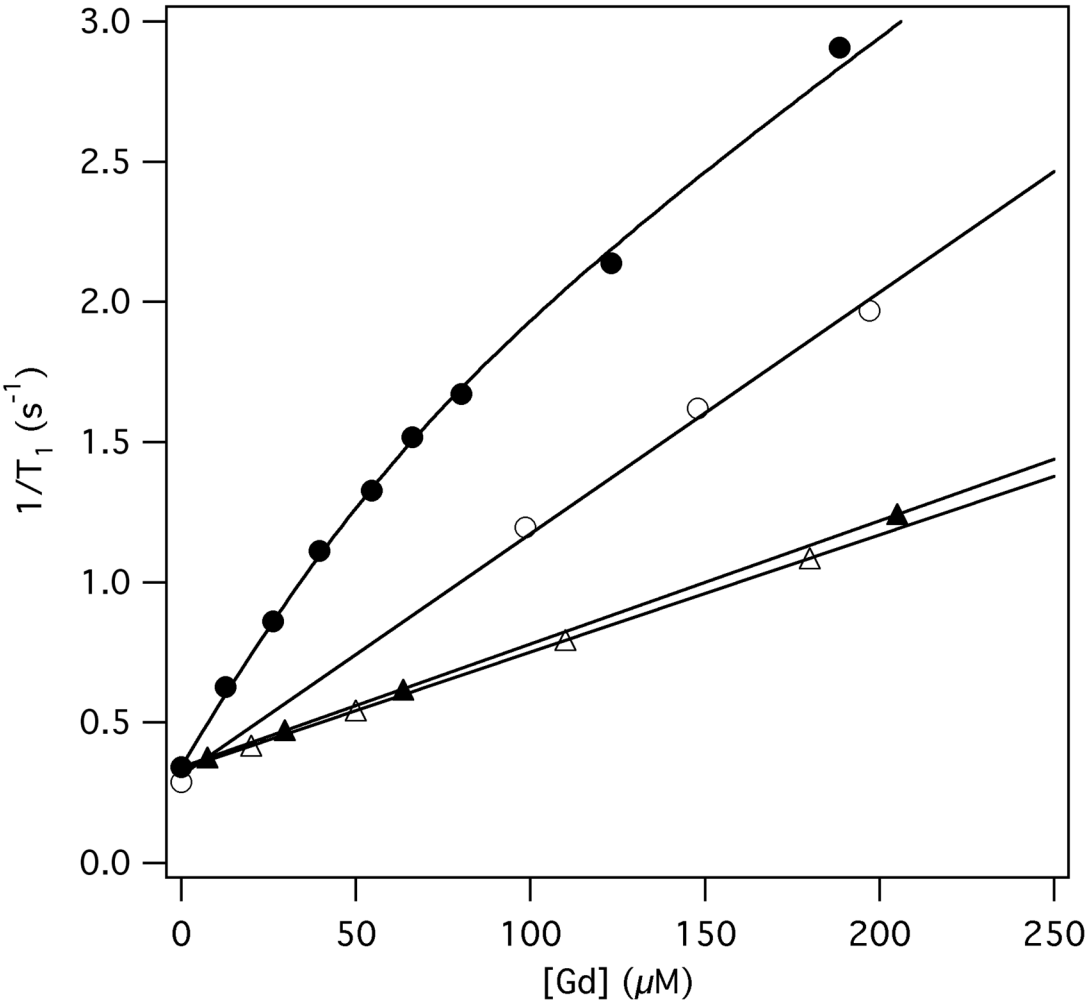

Figure 5.
Relaxation rate data for **Tn7-3a-Gd** (circles) and GdDTPA (triangles) in the presence (filled symbols) and absence (open symbols) of 30 μM fibrin. Solid lines are fits to the data as described in the text.

Table 1

Peptides and Peptide conjugates discussed in this work. Equilibrium dissociation (K_d) and inhibition (K_i) constants are given in micromolar (μM). Values in parentheses represent the number of equivalent binding sites, N_{bd}, obtained from the fit to the data.

Compound	Sequence	K_d (N_{bd}) Fibrin[a]	K_d (N_{bd}) DD(E)[b]	K_i DD(E)[c]
Tn6-1	WFHCPYDLCHIL	4.1±0.4 (2.3±0.1)	n.d.	3.1±0.4
Tn6-2a	WECPYGLCWIQ	2.9±0.2 (2.4±0.4)	0.85±0.03 (2.0±0.1)	0.9±0.2
Tn6-2b	QWECPYGLCWIQ	n.d.	n.d.	2.3±0.5
Tn6-2b-Fl	Fluor-Aca-QWECPYGLCWIQ	n.d.	0.057±0.006	n.d.
Tn6-1-Gd	GdDTPA-GG-WFHCPYDLCHIL	3.1±0.3 (2.3±0.1)	n.d.	2.2±0.2
Tn7-3	LPCDYYGTCLD	4.0±0.3 (2.1±0.05)	2.2±0.06 (1.9±0.1)	2.8±0.7
Tn7-3-Fl	Fluor-Aca-LPCDYYGTCLD	n.d.	1.3±0.4	n.d.
Tn7-3a-Gd	GdDTPA-LPCDYYGTCLD	6.9±0.8 (3.0±0.1)	n.d.	2.9±0.2
Tn7-3b-Gd	GdDTPA-GLPCDYYGTCLD	8.4±0.5 (1.8±0.1)	n.d.	3.9±0.3
Tn10-4	Ac-NHGCYNSYGVPYCDYS	8.7±1.5 (2.3±0.1)	3.0±0.1 (1.6±0.1)	3.5±0.3
Tn10-4-Fl	Fluor-AEGTGSNHGCYNSYGVPYCDYSAPG	n.d.	2.7±0.6	n.d

[a] direct binding to fibrin coated plate.

[b] direct binding to DD(E) measured by fluorescence anisotropy for Tn6-2b-Fl, Tn7-3-Fl, Tn10-4-Fl and by isothermal calorimetry for the other compounds.

[c] determined by inhibition of binding of the corresponding fluorescent probe, e.g. Tn6-1 inhibiting binding of Tn6-2b-Fl.

Table 2

Structural requirements for Tn6, Tn7 and Tn10 peptides, as determined by alanine scanning and DD(E) binding. Binding of Tn7 - Tn10 hybrid peptides are also presented. Data obtained by FP probe displacement assay using **Tn6-2b-Fl** (Tn6) and **Tn7-3-Fl** (Tn7 and Tn10). Standard errors were ≤10%.

Tn6-1	K_i (μM)	Tn6-2b	K_i (μM)	Tn7-3	K_i (μM)	Tn10-4	K_i (μM)
WFHCPYDLCHIL	3.1	QWECPYGLCWIQ	2.3	LPCDYYGTCLD	2.8	NHGCYNSYGVPYCDYS	3.5
AFHCPYDLCHIL	8.0	**A**WECPYGLCWIQ	--	**A**LCDYYGTCLD	3.1	NHGCYDSYGVPYCDYS	>100
W**A**HCPYDLCHIL	3.9	Q**A**ECPYGLCWIQ	4.3	L**A**CDYYGTCLD	2.9	NHGCYNYYGVPYCDYS	5.9
WF**A**CPYDLCHIL	3.3	QW**A**CPYGLCWIQ	6.2	LPC**A**YYGTCLD	5.9	NHGCYNYYGTPYCDYS	>500
WFHC**A**YDLCHIL	62	QWEC**A**YGLCWIQ	32	LPCD**A**YGTCLD	4.5	NHGCYDYYGTPYCDYS	>500
WFHCP**A**DLCHIL	16	QWECP**A**GLCWIQ	42	LPCDY**A**GTCLD	>100		
WFHCPY**A**LCHIL	16	QWECPY**A**LCWIQ	7.7	LPCDYY**A**TCLD	12		
WFHCPYD**A**CHIL	97	QWECPYG**A**CWIQ	93	LPCDYYG**A**CLD	>100		
WFHCPYDLC**A**IL	28	QWECPYGLC**A**IQ	4.3	LPCDYYGTC**A**D	15		
WFHCPYDLCH**A**L	19	QWECPYGLCW**A**Q	17	LPCDYYGTCL**A**	7.3		
WFHCPYDLCHI**A**	2.6	QWECPYGLCWI**A**	--	LPCDYYG**V**CLD	28		